Is the recent build-up of atmospheric CO 2 over Europe reproduced by models. Part 2: an overview with the atmospheric mesoscale transport model CHIMERE

C. Aulagnier, P. Rayner, Philippe Ciais, R. Vautard, L. Rivier, M. Ramonet

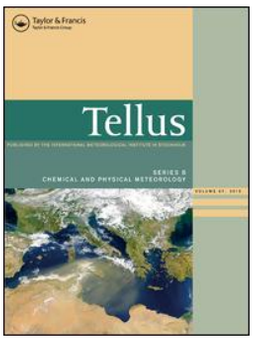

Tellus B: Chemical and Physical Meteorology

ISSN: (Print) 1600-0889 (Online) Journal homepage: https://www.tandfonline.com/loi/zelb20

Is the recent build-up of atmospheric CO_2 over Europe reproduced by models. Part 2: an overview with the atmospheric mesoscale transport model CHIMERE

C. Aulagnier, P. Rayner, P. Ciais, R. Vautard, L. Rivier & M. Ramonet

To cite this article: C. Aulagnier, P. Rayner, P. Ciais, R. Vautard, L. Rivier & M. Ramonet (2010) Is the recent build-up of atmospheric CO_2 over Europe reproduced by models. Part 2: an overview with the atmospheric mesoscale transport model CHIMERE, Tellus B: Chemical and Physical Meteorology, 62:1, 14-25, DOI: 10.1111/j.1600-0889.2009.00443.x

To link to this article: https://doi.org/10.1111/j.1600-0889.2009.00443.x

Published online: 18 Jan 2017.

Tellus
SERIES B
CHEMICAL
AND PHYSICAL
METEOROLOGY
PUBLISHED BY THE INTERNATIONAL METEOROLOGICAL INSTITUTE IN STOCKHOLM

Tellus (2010), 62B, 14–25
Printed in Singapore. All rights reserved

TELLUS

Is the recent build-up of atmospheric CO_2 over Europe reproduced by models. Part 2: an overview with the atmospheric mesoscale transport model CHIMERE

By C. AULAGNIER*, P. RAYNER, P. CIAIS, R. VAUTARD, L. RIVIER and M. RAMONET,
Laboratoire des Sciences du Climat et de l'Environnement, IPSL, CEA/CNRS/UVSQ, Paris, France

(Manuscript received 11 March 2009; in final form 17 August 2009)

ABSTRACT

In this issue, Ramonet et al. revealed a positive trend in European, atmospheric CO_2 concentrations relative to a marine, North Atlantic reference baseline, for the years 2001–2006. The observed build up mainly occurred during the cold season where it reaches a 0.8 ppm yr^{-1} at low-altitude stations to a 0.3 ppm yr^{-1} at mid-altitude stations. We explore the cause of this build-up using the mesoscale model CHIMERE. We first model the observed trends, using interannually varying fluxes and transport, then suppress the interannual variability in fluxes or aspects of transport to elucidate the cause. The run with no interannual variability in fluxes still matches observed trends suggesting that transport is the major cause. Separate runs varying either boundary layer height or winds show that changes in boundary layer height explain the trends at low-altitude stations within the continents while changes in wind regimes drive changes elsewhere.

1. Introduction

In the companion paper Ramonet et al. (2009) noted a significant increase in anomalous CO_2 concentrations over Europe since 2000. The evidence was a positive trend in the difference between concentrations at several European measuring sites and the Mace Head (western Ireland) station whose concentrations, when filtered to remove local influences, reflect concentrations over the North Atlantic. The trend was spatially robust, being reflected at most low to mid-altitude sites. It was, however, seasonally limited, being observed mainly in winter. The anomalous trend was twice to three times weaker at mid to high-altitude sites whose concentrations reflect hemispheric-scale structures. Thus the phenomena giving rise to the anomalous trend seem to be mainly localized over continental Europe, although a larger-scale underlaying mechanism cannot be excluded.

CO_2 concentration in the atmosphere arises from atmospheric transport acting on surface fluxes and chemical sources (there are no chemical sinks of CO_2 in the atmosphere). When both sources and transport have no interannual variability, resulting concentrations are a superposition of a constant trend and annual cycle. Deviations from such behaviour, for example, a change in the strength of the trends, imply a change in either sources, sinks or transport. Changes in spatial gradients noted by Ramonet et al. (2009) are among those origins, and must be clarified.

Separating the roles of fluxes and transport in the observed trends is both important and difficult. Several inverse studies like Gurney et al. (2002) and Rayner et al. (2008) have suggested that Europe is a significant biological carbon sink. But the European sink is not yet accurately quantified enough to evaluate changes in this term of the carbon budget. Furthermore, studies of European fossil fuel emissions (Marland et al., 2008) as a significant carbon source for Europe suggests relatively small changes in this term over the last decade. Thus, a significant trend in the net flux over Europe must come from other terms in the carbon budget, for example, from the ecosystem carbon balance.

A decadal change in fluxes would have implications for managing the European carbon cycle. It might even be an early indicator of global changes in northern extratropical carbon sink.

A decadal change in transport, however, has narrower implications for the carbon cycle, but is important for air quality, regional meteorological modelling and particularly for the conduct of future inversion studies. Since the coarse-scale studies of Dargaville et al. (2000) and Rödenbeck et al. (2003), it has been generally believed that interannual variations in transport were less important as drivers of concentration than changes in flux. Indeed several coarse-scale studies (Baker et al., 2006; Rayner et al., 2008) ignore changes in transport altogether. If we could show that such assumptions might cause serious errors in direct

*Corresponding author.
e-mail: celine.aulagnier@lsce.ipsl.fr
DOI: 10.1111/j.1600-0889.2009.00443.x

simulations, it would also guide how we performed inversions in future.

The aim of this paper, therefore, is to attribute the change in spatial gradient. We use the classical 'model laboratory' approach. First, we investigate whether we can simulate the observed behaviour. Given reasonable success, we then turn off various of the possible contributing causes. This is not a model validation study but it does form part of the evolution of an inversion system. A simple and coherent explanation of the observed trend will also increase our confidence in the model for upcoming inversion studies.

The outline of the paper is as follows. We begin with a short description of the experiment, in introducing the CHIMERE model, the driving fluxes, the sites for comparison, the model data selection, and the experimental setup. We then present the results focusing on the extreme seasons, winter and summer. Finally, we discuss the impact of such results on future inversions.

2. Experiment description

To test the role of fluxes versus transport changes in the observed trend, we carry out several simulations with the regional chemistry transport model CHIMERE (Schmidt et al., 2001; Bessagnet et al., 2004) over the period 2001–2006. The choice of a regional over a global model is motivated by intercomparisons such as Geels et al. (2007), Law et al. (2008) and Patra et al. (2008) which assess the capabilities of various transport models in matching high-frequency observations. Both studies find that high-resolution models perform better at fitting continental observations such as those used in Ramonet et al. (2009). The improved vertical and horizontal resolutions of these models mean they can better resolve both the boundary conditions (orography, etc.) and the dynamics. The CHIMERE model was among the best performed models in the precedent intercomparison study (Patra et al., 2008), so we have some confidence before applying it to this problem. It has also been shown to provide simulation or forecast skills allowing operational use for other species like ozone or aerosols (van Loon et al., 2007; Honoré et al., 2008). Here we use the CHIMERE model to transport CO_2 fluxes and radon (Rn-222) as a tracer of atmospheric transport processes.

2.1. The model description

The eulerian mesoscale chemical transport model CHIMERE (Schmidt et al., 2001) is a three-dimensional atmospheric transport model primarily designed to make long-term simulations for emission control scenarios. The model domain covers Western Europe at a horizontal resolution of 50 km by 50 km. We use 20 layers in the vertical on terrain following σ-coordinates, with seven layers in the lowest 300 m and the highest one around mid-troposphere. CHIMERE is an off-line model which requires mass-fluxes for transport calculations. These fluxes are provided by a run of the regional meteorological model MM5 (Grell et al., 1994) with output saved every hour. MM5 is nudged towards the analyses of the European Centre for Medium Range Weather Forecasting (ECMWF) every six hours. The CHIMERE model is a regional model which consequently requires boundary lateral and top conditions, which are supplied by a run of the global transport model LMDZ (Law et al., 2008; Hauglustaine et al., 2004) at daily frequency. For further information, see the model server http://euler.lmd.polytechnique.fr/chimere/.

2.2. The source functions

The source function for the biospheric CO_2 exchange was provided by the ORCHIDEE terrestrial biosphere model, which can simulate non-zero sources and sinks in the annual mean (Krinner et al., 2005) on a 3-hourly basis and at a 0.3° resolution. ORCHIDEE has also been shown to capture relatively well seasonal (Chevallier et al., 2006; Jung et al., 2007) and interannual (Vetter et al., 2008) variability of ecosystem CO_2 fluxes. The ORCHIDEE fluxes used to drive CHIMERE were forced by the meteorological analyses from the European Center for Medium Range Weather Forecasting (ECMWF). ORCHIDEE fluxes were interpolated to hourly time-steps and extrapolated to a 0.5° resolution on the CHIMERE grid to fit the requirements of CHIMERE. The ORCHIDEE fluxes used to drive LMDZ were driven by different forcing, namely the analyses from the Climate Research Unit (CRU) and the National Center for Environmental Prediction (NCEP). The resulting LMDZ concentrations are only used for the CHIMERE boundary conditions and tests showed negligible sensitivity of the relative CO_2 trends to these boundary conditions. Consequently, we are confident this inconsistency will have no impact on the resulting trends.

The source function for the air–sea CO_2 exchange is based on monthly estimates following the surface pCO_2 climatology from (Takahashi et al., 2002) and the air–sea gas exchange parametrization from (Wanninkhof, 1992). These were also interpolated to hourly time-steps and from a 2.5° resolution to the CHIMERE gridsize 0.5° resolution, to fit the requirements of CHIMERE.

The source function for fossil CO_2 emissions was derived from the EDGAR fast-track product (van Aardenne et al., 2005). It has spatial and temporal structures pertaining to the year 2000. It provides fossil fluxes at an hourly time-step resolution and at a 1.0° spatial resolution. Annual totals have been rescaled according to country level fossil estimates of the Carbon Dioxide Information Analysis Center (CDIAC), for each year except for the years 2005 and 2006 for which the data were not yet available. For these years a global rescaling has been applied following the estimates of Canadell et al. (2007), that is 8.15 and 8.4 GtC per year, respectively. The resulting fluxes were then interpolated on the 0.5° CHIMERE grid.

Table 1. Typology and location of the study sites

Site	Type	Location	Model level	Data	
				Measurements	Selection
MHD	Ground-based	Western coast of Ireland 53°20′N–9°54′W–25m asl	1	Continuous	Wind-based
HUN	Tall-tower	Western plains of Hungary 46°57′N–16°39′E–248m asl	5	Continuous	Afternoon 12–16 UTC
BAL	Grab-sampling onboard a ferryboat	Sailing around the Poland coast 55°21′N–17°13′E–3m asl	1	Once a week	None
SCH	Ground-based	Eastern alps of Switzerland 47°55′N–7°55′E–1205m asl	11	Continuous	Nighttime 22–06 UTC
PUY	Ground-based	Central massif of France 45°46′N–2°58′E–1465m asl	11	Continuous	None
PRS	Ground-based	Western alps of Italy 46°56′N–7°42′E–3480m asl	14	Continuous	None
ORL	Grab-sampling onboard an aircraft	Flying over a French Forest 47°50′N–2°30′E–2000/3000 m agl	10/15	Twice a month	None

Notes: We also give the model level retained to fit the altitude of the sites. We summarize the data measurements and selection for each site, actually the same as in Ramonet et al. (2009).

The source function for radon emissions is a very simple one as it is equal to zero milliBecquerel per square metre per second over ocean and equal to one milliBecquerel per square metre per second over land as in Jacob et al. (1997). This may be too simple (Szegvary et al., 2007) to reproduce accurately the observed radon concentrations but is sufficient to probe the relationship between trends in boundary layer depth and concentrations within the model. Indeed by transporting a constant radon source function which is neither seasonally nor diurnally dependent we should be able to isolate the effects of transport on long-term trends in concentrations especially the effects of vertical mixing. The short lifetime of radon also allows us to isolate the effects of local to regional transport from large-scale advection.

2.3. The study sites

For detailed site location and data selection see Table 1.

The establishment of a reference, marine baseline is critical if one wants to attribute changes in spatial CO_2 gradients to changes in European atmospheric dynamics or fluxes. We choose the Western Ireland, coastal station Mace Head (MHD) as the reference for European gradients. This station alternatively receives maritime air masses from the Atlantic Ocean, and continental air masses exposed to sources from Western Europe. We only retain the simulated CO_2 concentrations advected by air masses from the North Atlantic sector, as done by Bousquet et al. (1996) and Ramonet et al. (2009) with observations. We use approximately the same selection criteria in the model as Ramonet et al. (2009) used with observations, namely a wind direction from between 200° and 300°, and a local, minimal wind speed of 4 $m\,s^{-1}$ as in Bousquet et al. (1996). This selected time-series is gap-filled and smoothed using the methods described below and spatial gradients are calculated by subtracting this selected, smoothed series from similarly treated series at other sites. These gradients will be denoted ΔCO_2.

We consider 6 sites within Europe, comprising tall towers, mountain sites, continental and coastal stations. The ground-based, mountain stations are particularly useful to assess the long-term trends in ΔCO_2, as they are less sensitive to short-term variability of surface emissions. However they are also more difficult to model because of a more complex mixture of transport. When sampling model fields to compare with observations, we extract the nearest CHIMERE model gridpoint and level to the given station locations. We apply the same data set selection as Ramonet et al. (2009). We also smooth the selected data, fitting the retained data by applying a low-pass filter with the same cut-off frequencies as Ramonet et al. (2009), using the curve-fitting routines described by Thoning et al. (1989).

2.4. The considered scenarios

We first consider a control case in which we simulate the European spatial gradients with our best estimates of the fluxes and transport for each year. This control case denoted A-scenario focuses on the coupling of fluxes and transport, both variables, to simulate the observed changes in spatial gradient from Ramonet et al. (2009). Only if the simulation of the observed changes in spatial gradient from Ramonet et al. (2009) are reasonable can we use the model to choose among possible causes. We then consider further scenarios.

In the B-scenario the observed ΔCO_2 trends reflect changes in atmospheric transport only. Here the aim is to test ΔCO_2 changes due only to transport changes. We therefore run CHIMERE over

the years 2001–2006 with the same set of surface fluxes for each year of the simulation, namely the ORCHIDEE and EDGAR fluxes which pertain to the year 2002. The choice of year for fluxes is not important for deciding whether interannual transport drives significant continental trends since, as pointed out in the introduction, annually repeating transport and fluxes cannot drive such a trend. However the choice of year for fluxes may well affect the strength of the trends so we repeat the analysis with fluxes for 2005. We did not use a climatology of fluxes since this would suppress synoptic variability which could turn out to interact with transport variability. We also transport radon under the same transport scenario. We further subdivide this scenario. We expect winds and boundary layer heights to be the key parameters controlling the trends in atmospheric composition. We test this by running CHIMERE with interannually variable winds and boundary layer heights, versus interannually variable winds and annually repeating boundary layer heights versus annually repeating winds and boundary layer heights. Note the inconsistency between annually repeating (winds and) boundary layer heights and other interannually variable parameters.

Obviously we cannot rule out with A- and B-scenario that a non-modelled trend in surface continental fluxes may explain the observed ΔCO_2 trend as well as trends in winds or boundary layer heights do.

(i) Increasing CO_2 concentrations at continental level could arise from a slow-down of the CO_2 uptake by vegetation in response to climate change. Indeed, European primary productivity has been drastically reduced in 2003 because of the heat and drought (Ciais et al., 2005; Vetter et al., 2008), and there is evidence of longer-term changes at higher latitudes (Piao et al., 2008).

(ii) Increasing CO_2 concentrations at rural, low altitude stations could arise from increasing fossil fuel emissions or from regional shifts in the distribution of fossil fuel emissions. But fossil fuel emissions have been roughly stable in most European countries over 2001–2006. Yet although trends in sectorial emissions were significant over 1990–2004 they were quite negligible over 2001–2006. For instance in France, transports and residual emissions increased by 22% while industrial emissions decreased by 22% over 1990–2004, changes in the same sectorial emissions were less than 5% over 2001–2006 according to the United Nations Framework Convention on Climate Change (UNFCC).

At the continental level neither ORCHIDEE fluxes nor EDGAR fossil estimates displayed any such trends nor shifts anyway. As a consequence fluxes alone (i.e. with constant transport) cannot force trends in the modelled ΔCO_2.

3. Results

3.1. At Observations sites

Figure 1 shows the mean winter and summer ΔCO_2 simulated by CHIMERE at six European stations—among those studied by Ramonet et al. (2009)—with an interannually variable source function. Figure 2 shows the resulting trends over the 2001–2006 time period, with two different, interannually recycled source functions, plus the observed trends over the same time period. Table 2 summarizes modelled and observed trends and related uncertainties.

In the control case, A-scenario, in winter, we can divide the sites into three groups from Fig. 1. First, the low-altitude stations (HUN, BAL) which present a large positive ΔCO_2 (+7 ppm) and a strong interannual variability ($\leq +4$ ppm). Second, the mid-altitude stations (SCH, PUY) which show a small positive ΔCO_2 (+2 ppm) and less interannual variability ($\leq +2$ ppm). Third, the high-altitude stations (ORL, PRS) with a small negative ΔCO_2 (−2 ppm) and the same small interannual variability ($\leq +2$ ppm) as mid-altitude stations. All these stations display a linear increase of ΔCO_2 between winters 2002 and 2005, with a decrease in winter 2006.

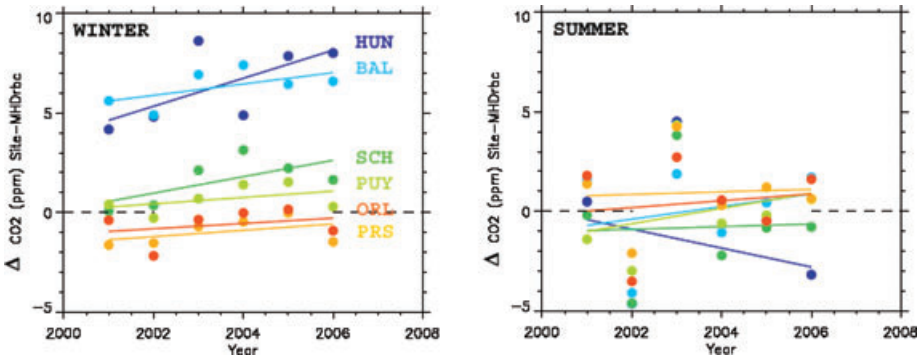

Fig. 1. Winter and summer spatial CO_2 gradients (denoted ΔCO_2) for six European stations with variable source functions, from 2001 to 2006. Gradients are related to MHD under marine conditions (denoted MHD_{rbc}). The left-hand plot displays winter gradients by CHIMERE and the right-hand plot displays summer gradients. All gradients are given in ppm.

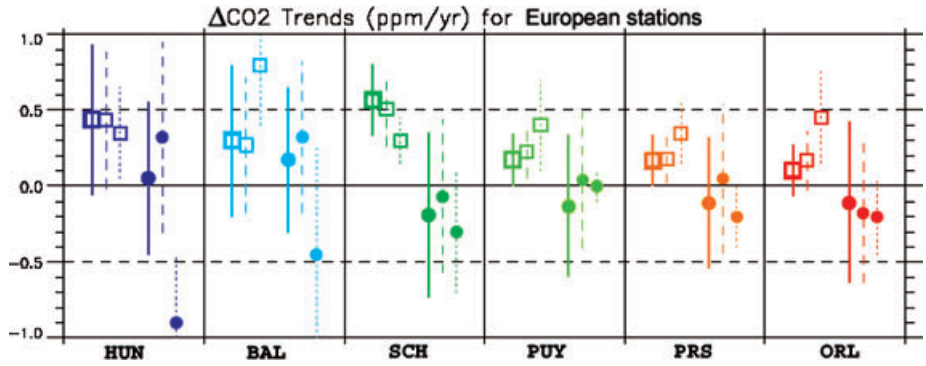

Fig. 2. Winter and summer 2001–2006 ΔCO_2 trends for six European stations. These trends result from a linear interpolation of the gradients seen in Fig. 1. Each trend is given with its 1σ uncertainty, both in ppm by year. Winter trends are marked by a square and summer trends by a round. For each season and each station we give three trends, by order, from left- to right-hand side: (1) the ones simulated by CHIMERE with interannually recycled 2002 source function; (2) the ones simulated by CHIMERE with interannually recycled 2005 source function and (3) the ones observed by Ramonet et al. (2009). For (1), (2) and (3) the associate 1σ uncertainty is, respectively, fitted in full lines (1), in dashed lines (2) and in dotted lines (3).

Table 2. Winter and summer trends in atmospheric CO_2 CHIMERE concentrations for six continental, European stations related to the MHD marine station

Site	DJF Trends (1σ uncertainty) in [CO_2]			JJA Trends (1σ uncertainty) in [CO_2]		
	Obs	Mod		Obs	Mod	
		–	2002		–	2002
HUN	0.35 (0.30)	0.70 (0.40)	0.45 (0.50)	−0.90 (0.45)	−0.50 (1.00)	0.05 (0.50)
BAL	0.80 (0.40)	0.30 (0.20)	0.30 (0.50)	−0.45 (0.70)	0.30 (0.60)	0.20 (0.50)
SCH	0.30 (0.15)	0.45 (0.20)	0.55 (0.20)	−0.30 (0.40)	0.05 (0.70)	−0.20 (0.50)
PUY	0.40 (0.30)	0.20 (0.20)	0.20 (0.20)	−0.00 (0.10)	0.40 (0.60)	−0.15 (0.45)
PRS	0.35 (0.20)	0.20 (0.20)	0.20 (0.20)	−0.20 (0.20)	0.05 (0.55)	−0.10 (0.40)
ORL	0.45 (0.30)	0.20 (0.20)	0.15 (0.20)	−0.20 (0.25)	0.20 (0.60)	−0.10 (0.60)

Notes: Each trend is given with its 1σ uncertainty, both in ppm by year. We compare observed trends with a couple of modelled ones corresponding to different source functions, an interannually variable source function (column denoted –) and an interannually constant source function taken equal to the 2002 source function (column denoted 2002).

The CHIMERE model simulates well the observed positive winter trends in ΔCO_2 at all continental sites within the 1σ uncertainty in each trend (cf. Fig. 2). The simulated trends show little sensitivity to the source function, whether it is annually recycled or variable. This first result suggests that winter trends are transport driven rather than flux driven, in agreement with B-scenario. In the following (Part 3.2), we will consequently focus on the winter trends resulting from the transport of recycled fluxes, using 2002 fluxes unless notified.

Unlike winter, summer gradients do not change systematically with location or altitude (cf. Fig. 1). This is a consequence of (1) the efficiency of transport processes which mix air masses more vigorously over land, thus weakening the spatial gradients between ocean and continents and between the free troposphere and the boundary layer and (2) the fact that in summer the sinks now balance the sources so the net fluxes emitted to the atmosphere are very small over a day (not shown) so the eventual decrease (increase) of the boundary layer heights can not concentrate (dilute) the small flux signal. All stations display the same features in ΔCO_2, a small ΔCO_2 of -1 to $+1$ ppm and a strong interannual variability of $+6$ ppm so that no clear trend can be established even for the control case, A-scenario. In particular, summer 2003 stands out as a positive anomaly in keeping with the results of Ciais et al. (2005) and summer 2002 stands out as a negative anomaly. CHIMERE does not reproduce the summer negative ΔCO_2 trends observed at the two low altitude stations HUN and BAL.

Regarding Figs. 1 and 2, CHIMERE simulations demonstrate the same combination of weak trends and large interannual variability as the observations. The model also simulates strong climate related anomalies in 2002—abnormally wet—and 2003—abnormally hot and dry—in agreement with Ramonet et al. (2009). That study already noted that observed spatial gradients were especially high when droughts occurred, in 2003. In summary, ΔCO_2 is much smaller in absolute value and much more variable in summer than in winter and more closely linked

Table 3. Winter trends in 24-h mean atmospheric CO_2 and radon CHIMERE concentrations for six European regions related to MHD station

Zone	Trends in [CO_2]						Trends in [Rn]		
	–		BLH		BLH, Winds		–	BLH	BLH, Winds
	2002	2005	2002	2005	2002	2005			
1. North-Western Europe Irlande, UK, Northern sea	0.00	0.00	−0.20	−0.25	−0.35	−0.35	−0.05	−0.10	−0.10
2. Southwestern Europe Spain, Atlantic sea	0.45	0.40	0.35	0.25	−0.20	−0.20	0.20	0.10	−0.05
3. Mediterranean Italy, Mediterranean sea	0.25	0.20	0.25	0.25	−0.20	−0.20	0.00	0.00	−0.05
4. Western Europe France, Western Germany	0.95	0.60	0.45	0.25	−0.25	−0.25	0.15	0.00	−0.05
5. Central Europe	0.30	0.20	0.00	−0.15	−0.30	−0.30	0.00	−0.10	−0.10
6. Eastern Europe	0.50	0.45	0.25	0.15	−0.20	−0.20	0.00	−0.05	0.00

Notes: Trends in ΔCO_2 concentrations are given in ppm by year and trends in ΔRn concentrations are given in 10^6 Becquerel per metre cubed by year. We give modelled trends issued from three different meteo drivers configurations: (1) interannually variable winds and boundary layer heights (column denoted –) (2) interannually variable winds but interannually recycled boundary layer heights, from 2001 (column denoted BLH) (3) interannually recycled winds and boundary layer heights, from 2001 (column denoted BLH,Winds). So the parameter(s) kept constant throughout the years of the simulation give its (their) name(s) to the column. We also give modelled trends issued from two different source functions: (1) an interannually constant source function taken equal to the 2002 source function (column denoted 2002) and (2) an interannually constant source function taken equal to the 2005 source function (column denoted 2005). So the ΔCO_2 trends sensitivity to the CO_2 fluxes intraseasonality is tested. The six regions for which we calculate the mean local trends have been determined in regards of their similarities in terms of fossil fuel emission rates, vegetation types, and synoptic atmospheric patterns, that is, Depression/Island, Anticyclone/Acores, etc. Another condition for gridpoints to be in the same region is to display quite the same trends than their surroundings.

to flux changes. The fluxes themselves are sensitive to seasonal climate anomalies.

3.2. Over European regions

Table 3 summarizes modelled winter trends in 24-h mean ΔCO_2 and ΔRadon for six European regions delimited by their similarities, for example, same surface type and/or same synoptic atmospheric pattern, for two different source functions (2002 and 2005), both interannually constant, and for three different configurations of meteorological forcing, which are detailed in the three following sections.

3.2.1. Interannual BLH and Winds. Figures 3–6, respectively, display mean 2001–2006 winter trends in 24-h mean ΔCO_2, ΔRn, boundary layer height (BLH) and wind speed, plus associated 24-h mean 2001–2002 winter ΔCO_2, ΔRn, boundary layer height and wind speed. Figures 3 and 4 only display winter trends within the lowest 300 m of the atmosphere resulting from the transport of recycled fluxes, B-scenario.

Positive ΔCO_2 winter trends are simulated within the 0–300 m layer, over the Western part of the domain—including Spain, France, Switzerland and Western Germany—along with areas in Eastern and Central europe (cf. Fig. 3). Trends in the first two regions are statistically significant at the 1σ level. Trends over Western Germany are maximal and around +1 ppm yr^{-1}. Positive ΔCO_2 trends of 0.2 ppm yr^{-1} are also simulated everywhere within the 1000–3000 m layer (not shown). Positive ΔRn trends are simulated over Spain, France, Atlantic coast and over a small part of southeastern Europe (cf. Fig. 4). Negative trends in boundary layer heights and wind speeds are simulated over the same areas, about −35 m yr^{-1} and −0.5 m s^{-1} yr^{-1} from Figs. 5 and 6, respectively.

No negative ΔCO_2 trends are simulated (cf. Fig. 3) while negative ΔRn trends are simulated over the Mediterranean Sea, the Italian coast, the Northern UK and North sea (cf. Fig. 4). Positive trends in boundary layer heights are simulated over the same areas, about +40 m yr^{-1} from Fig. 5. Positive trends in wind speeds are also simulated over the Mediterranean Sea, the UK and North sea, with a maximum increase of +0.8 m s^{-1} yr^{-1} from Fig. 6.

There is a strong spatial correlation between positive (negative) trends in ΔCO_2 concentration (cf. Figs. 3 and 4) in the lower

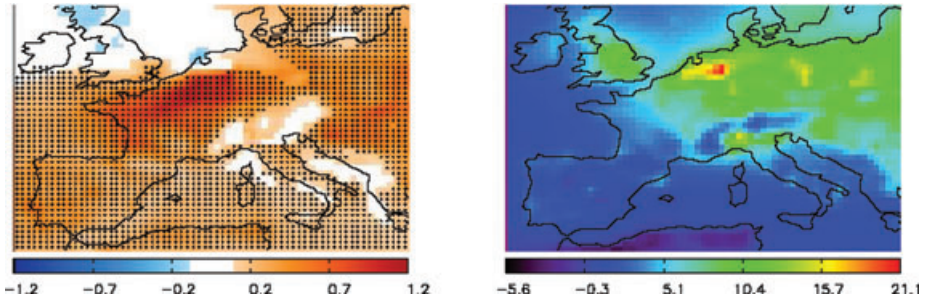

Fig. 3. Mean 2001–2006 winter trends in 24-h mean ΔCO_2 (left-hand panel) and 24-h mean 2001–2002 winter ΔCO_2 concentrations (right-hand panel) over Europe, within the first hundred metres of the atmosphere. Concentrations have been averaged between 0 and 300 m before producing mean seasonal gradients and calculating linear trends. Fluxes of year 2002 have been recycled over the years. Trends are given in ppm by year, ΔCO_2 in ppm. The dotted areas are assigned to statistically significant trends.

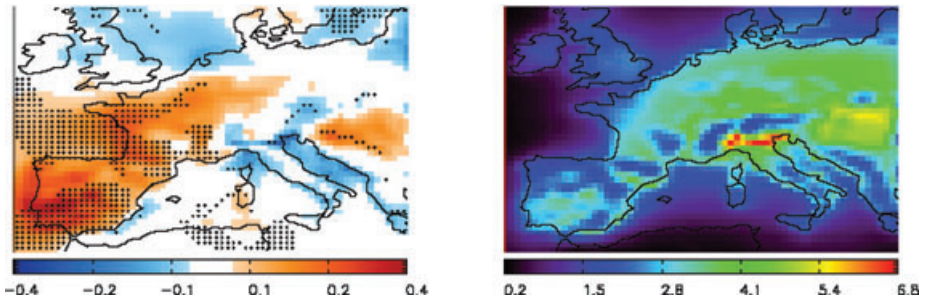

Fig. 4. Mean 2001–2006 winter trends in 24-h mean ΔRn (left-hand panel) and 24-h mean 2001–2002 winter ΔRn concentrations (right-hand panel) over Europe, within the first hundreds metres of the atmosphere. Concentrations have been averaged between 0 and 300 m before producing trends. Trends are given in 10^6 Becquerel per metre cubed by year, ΔRn in 10^6 Becquerel per metre cubed. The dotted areas are assigned to statistically significant trends.

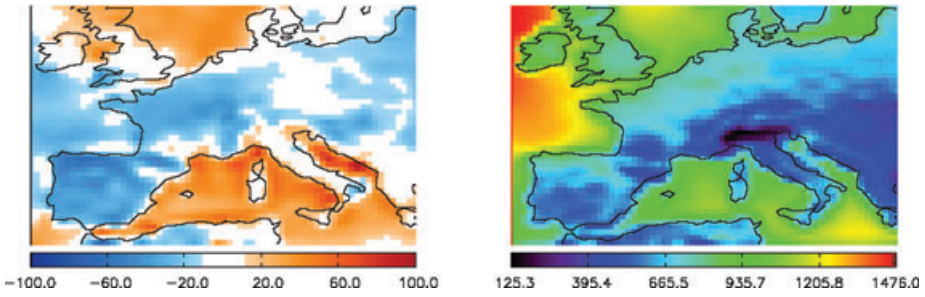

Fig. 5. Mean 2001–2006 winter trends in 24-h mean boundary layer height (left-hand panel) and 24-h mean 2001–2002 winter boundary layer heights (right-hand panel) over Europe. Trends are given in metres by year, 24-h mean heights in metres.

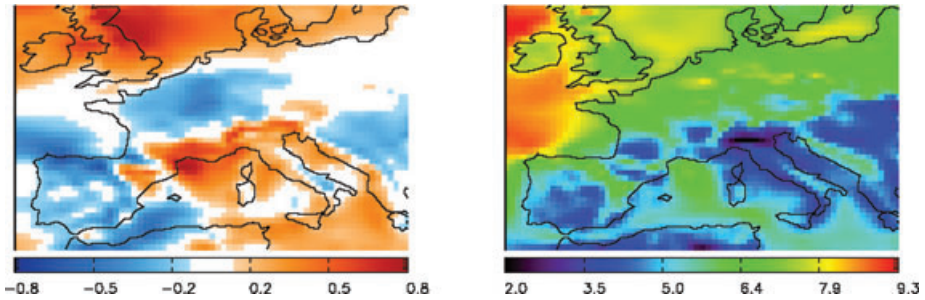

Fig. 6. Mean 2001–2006 winter trends in 24-h mean wind speed (left-hand panel) and 24-h mean 2001–2002 winter wind speeds (right-hand panel) over Europe. Trends are given in metres per second by year, 24-h mean wind speeds in metres per second.

atmosphere and negative (positive) trends in boundary layer height (cf. Fig. 5). The correlation is nearly perfect for radon and strong for CO_2. The main exception is over the Mediterranean where both ΔCO_2 and BLH increase. There is also a spatial correlation between trends in ΔCO_2 concentration (cf. Figs. 3 and 4) in the lower atmosphere and trends in wind speed but partly (cf. Fig. 6) because of trends in BLH and wind speed being obviously spatially correlated (cf. Figs. 5 and 6), as the BLH is uprise by wind-shear during cold, winter seasons.

We tested that the boundary conditions set-up from LMDZ do not affect the simulated ΔCO_2 trends inside the domain. In particular, we ran an experiment with CO_2 equal to 0 as boundary condition, i.e. incoming air masses being CO_2-free. The resulting trends within the domain were still the same than those displayed by Fig. 3 with a realistic boundary condition. This experiment has allowed us to rule out an external (i.e. outside Europe) cause to the observed ΔCO_2 trends.

We also investigated relationships with several other meteorological parameters (e.g. temperature, humidity) but noticed no strong relationships. We thus expect the trends in BLH and/or winds to be driving the winter trends in ΔCO_2 and ΔRadon concentrations. In particular, we expect the decrease (increase) of the boundary layer height to act locally to concentrate (dilute) nearby emissions, since, in winter, the net source is positive except maybe over Mediterranean continental regions where Mediterranean ecosystems take up CO_2 more than they release. The short lifetime of radon means this local effect would be the only important mechanism for this gas and would explain the good spatial anti-correlation between Figs. 4 and 5.

Conversely, CO_2 can be transported long distances. So looking back at Fig. 3 over the Mediterranean—where the CO_2 fluxes are small compared to continental ones and where both ΔCO_2 and BLH increase—we suspect the increase in ΔCO_2 concentrations might arise from advection of elevated ΔCO_2 concentrations from the continent. These elevated ΔCO_2 concentrations over the continent are expected from the decrease in continental boundary layer heights displayed by Fig. 5.

3.2.2. Recycled BLH and interannual winds. Figure 7 shows the mean 2001–2006 winter trends in 24-h mean ΔCO_2 with recycled BLH and interannual winds, plus the mean 2001–2006 winter trends in 24-h mean ΔCO_2 induced by trends in BLH.

Driven with interannually variable winds but recycled boundary layer heights, CHIMERE now simulates weaker positive to slightly negative trends in surface concentrations (cf. Fig. 7) and still the same positive trends higher in the atmosphere (not shown).

At low altitude (0–300 m), recycling the boundary layer heights does not change the global patterns but shifts them negatively, the more within the continent, for example, over France, Germany and Eastern countries. Thus, we get weaker positive trends over Western and Eastern Europe, no trends over Central Europe, and negative trends over North-Western Europe. Negative trends in BLH explain (1) large part of the lower layer positive trends in ΔCO_2 continental Europe except near Mediterranean areas and (2) whole part of the lower layer positive trends in ΔRn over continental Europe except over South Spain (not shown). This supports our hypothesis that the decrease of the continental boundary layer height acts locally on concentrating nearby emissions. However the decrease of the continental boundary layer height does not explain large-scale patterns of the lower layer positive trends. Indeed, the lower layer positive trends in ΔCO_2 over Mediterranean, Atlantic and continental near Mediterranean areas (e.g. Spain where the decrease of the boundary layer is also strong) remains unchanged by recycling the boundary layer heights.

At higher altitudes (1000–3000 m), recycling the boundary layer heights does not have any effect on the simulated positive trends (not shown), suggesting either that these responses are decoupled from the lower level trends or that they are the result of changes in vertical motion which are not simulated in this case. We also note from Fig. 5 that the mean BLH of 500–700 m lies below the 1000–3000 m layer we are discussing so that reductions in BLH would not be expected to influence the

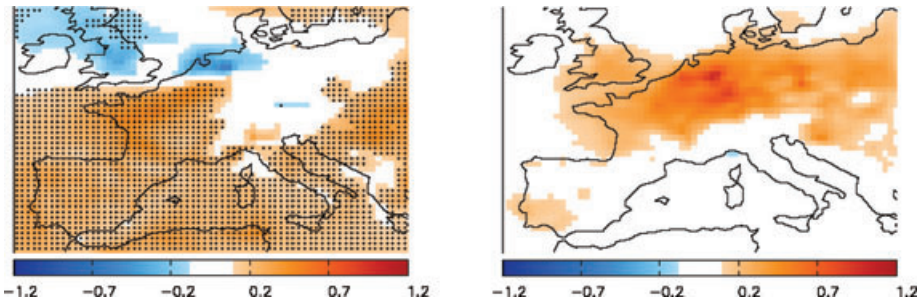

Fig. 7. Mean 2001–2006 winter trends in 24-h mean ΔCO_2 after recycling 2001 boundary layer heights over the years (left-hand panel) and mean 2001–2006 winter trends in 24-h mean ΔCO_2 induced by trends in boundary layer heights (right-hand panel), calculated by subtracting the mean trends displayed by recycled boundary layer heights and interannually variable winds (this figure, left-hand panel) from the mean trends displayed by interannually variable boundary layer heights and winds (Fig. 3, left-hand panel). Both trends are given in ppm by year and result from a linear interpolation between spatial gradients within the first hundreds metres. The dotted areas are assigned to statistically significant trends.

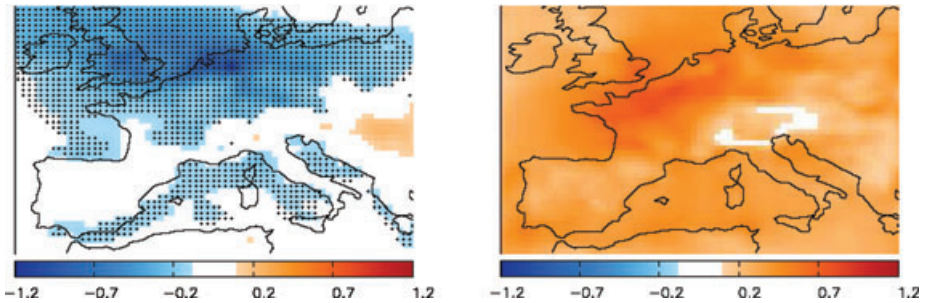

Fig. 8. Mean 2001–2006 winter trends in 24-h mean ΔCO_2 after recycling 2001 boundary layer heights and winds over the years (left-hand panel) and mean 2001–2006 winter trends in 24-h mean ΔCO_2 induced by changes in winds (right-hand panel), calculated by subtracting the mean trends displayed by recycled boundary layer heights and winds (this figure, left-hand panel) from the mean trends displayed by recycled boundary layer heights and interannually variable winds (Fig. 7, left-hand panel). Both trends are given in ppm by year and result from a linear interpolation between spatial gradients within the first hundreds metres. The dotted areas are assigned to statistically significant trends.

concentrations much. What affects the upper layers should be a larger scale process.

3.2.3. Recycled BLH and winds. Figure 8 shows the mean 2001–2006 winter trends in 24-h mean ΔCO_2 with recycled BLH and winds, plus the mean 2001–2006 winter trends in 24-h mean ΔCO_2 induced by changes in winds.

Driven with recycled boundary layer heights and winds, CHIMERE now simulates slightly negative trends throughout the domain, at both low and higher levels. From Fig. 8 negative trends at low level are stronger over Northern Europe, North sea and the Netherlands.

Recycling the BLH and winds affect the trends within the whole domain, that is, within the lower layers (cf. Fig. 8) and within the upper (not shown). Interannual variability in winds is thus responsible for (1) what is left of the lower layer positive trends in ΔCO_2 continental, north Europe and (2) whole part of the lower layer positive trends in ΔCO_2 southwest Europe, and seas, for example, Mediterranean. Considering we are close to the Anticyclonic system of the Azores, and that in Anticyclonic systems, wind speeds are often reduced, so that CO_2 concentrations get higher, a decrease in already reduced wind speeds (cf. Fig. 6) may generate an increase in already enhanced CO_2 concentrations.

More importantly, the trends in BLH and winds altogether explain all of the observed positiveness of the trends in ΔCO_2 and ΔRn concentrations. The upper layer trends are also now everywhere negative. Thus it appears interannual variability of winds plays an important role in these trends. The mechanism by which the trends in winds affect the upper layers is not clear at the moment. Still it may be linked to depressionary systems and associated cold frontal features. Finally, note that modelled trends in BLH and wind speed are generally correlated because of the BLH being uprise by wind-shear during cold, winter seasons so that modelled BLH and wind speed are partly dependent from each other through the frequency of weather regimes.

It is difficult to separate the impacts of trends in BLH and winds on ΔCO_2 due to the strong relationship between these forcing factors. Partial correlation analysis yields little relationship between trends in ΔCO_2 and trends in either BLH or wind speed once the effect of the other forcing has been removed. This strong dependence of the two forcings also explains why the trend in ΔCO_2 is less than the sum of the trends from the two separate experiments (cf. Fig. 8).

4. Discussion

4.1. The role of fronts

Fronts play an important role in vertically redistributing the boundary layer content (Eckhardt et al., 2003). Chan et al. (2004) and Lokoshchenko and Elansky (2006) already showed that chemical composition of tropospheric air is strongly coupled to atmospheric dynamic. Indeed, in the absence of significant synoptic scale circulation, the boundary layer has minimal exchange with the free troposphere, leading to strong CO_2 gradients across the top of the boundary layer in the presence of significant net fluxes (Chan et al., 2004). Whereas in the presence of synoptic scale frontal circulation, the boundary layer content can be moved upward to the mid to upper troposphere, leading to strong CO_2 gradients across the frontal regions. Moreover, intense advection of cold air at the rear of the cyclone—through the cold conveyor belt—can lead to the development of an unstable stratification in the nighttime atmospheric boundary layer (Lokoshchenko and Elansky, 2006). So can it be done through the warm conveyor belt (Eckhardt et al., 2003).

This is coherent with the observed and modelled trends at SCH fitted with only the nighttime data (cf. Fig. 2) when the vertical mixing is reduced—except during frontal passages—and the mountain top lies above the mixed boundary layer. This is also coherent with the modelled trends in the free troposphere which are not sensitive to changes in the boundary layer heights, but really dependent to changes in wind speeds (and directions). The only large-scale process able to uplift air masses recently exposed to surface emissions up to the 1000–3000 m layer is the large-scale upward motions occurring with fronts (Eckhardt et al., 2003; Lokoshchenko and Elansky, 2006), breaking the

established, strong gradient between the free troposphere and the boundary layer.

An open question is whether the change in mixing is related to a lower frequency or a lower intensity of cold fronts passage, whether infrequent, strong mixing has a bigger effect or a smaller one than frequent but weaker. Matulla et al. (2007) claim that Europe's storm climate has undergone significant changes throughout the last century and comprises significant variations on a decadal timescale, and Smits et al. (2005) already noted on a smaller scale, trends in storminess over the Netherlands. Still they did not agree on the sign of the trends, finding a decreased storminess over the Netherlands while the Centre for Medium-Range Weather Forecasts reanalysis data suggest increased storminess over Northern Europe during the same 40 yr period (Smits et al., 2005). Another question is whether there is a relationship between the behaviour of fronts and the North Atlantic Oscillation (NAO). The capability of the NAO index to assess changes in cyclone activity across Europe varies in space and with the considered period (Matulla et al., 2007) so that no clear relationship could be established between the NAO and the frequency of storms.

4.2. The differences between meteo models

There are some differences between the trends displayed by MM5 boundary layer heights and the ones displayed by ECMWF boundary layer heights (Ramonet et al., 2009). Between winters 2001 and 2006, MM5 daily mean boundary layer heights decreased about −35 m per year over Southwestern and Eastern Europe while ECMWF daily mean boundary layer heights did not (Ramonet et al., 2009). However, decreases in nocturnal mean BLH were about the same for both models (-30 m yr^{-1}). Another similarity is the increase in 24-h mean BLH over Mediterranean, displayed both by MM5 ($+35$ m yr^{-1}) and ECMWF ($+50$ m yr^{-1}).

The differences between the meteorological models suggest some caution in attributing the trends in ΔCO_2 largely to transport processes, particularly trends in BLH. The differences also require explanation and, more importantly, an independent observational test. The best data for such a test are probably the measurements of BLH by radiosonds. There might also be a role for measurements of radon in the boundary layer although their interpretation is complicated by climate-related changes in radon source.

In the framework of a future inversion, we should keep in mind that there are some uncertainties related to long-term transport modelling, and we should quantify them then take into account these uncertainties through long-term inversion (Lin and Gerbig, 2005). If not we may inadequately attribute a change in CO_2 concentrations to a change in CO_2 sinks or emissions when it corresponds to a change in transport-induced CO_2 air-masses distribution.

5. Conclusion

Atmospheric CO_2 concentration varies in response to sources and sinks and to synoptic air mass transport. Estimating global carbon sources and sinks by inverting atmospheric CO_2 concentrations through the use of a mesoscale, atmospheric transport model consequently requires to preliminary investigate (1) the implication of transport processes in controlling the long-term variability, past and possible future trends of the atmospheric composition and (2) the capacity of the model to successfully reproduce part of these processes. This article follows a data analysis by Ramonet et al. (2009) which assesses the recent build-up of atmospheric CO_2 over continental Europe in winter, displayed by all continental observation sites except free tropospheric sites. The marine observation site Mace Head has been taken as a reference. The contribution of transport versus sources to the observed signals has been investigated using the CHIMERE model. The role of variations in fluxes, large-scale winds and boundary layer heights in simulating the observed trends has been investigated by systematically recycling these variables.

The conclusions of the study can be summarized as follows:

(i) The model reproduces the winter build-up in European CO_2 despite the lack of trends in the fluxes. This suggests that the build-up is not necessarily the result of changes in underlying fluxes. Modelled and observed build-up are both stronger in winter and at low altitudes.

(ii) The simulated, winter CO_2 and Rn build-up persist even when the flux from only one year is repeated. This suggests that the observed build-up is a result of changes in transport not fluxes. This also suggests that even in case of a stabilization of emissions, changes in transport-induced CO_2 air-masses distribution can generate such a build-up over European-sized regions.

(iii) The winter build-up at low-altitude continental stations is reduced by about 60% when boundary layer heights from only one year are used. There is also a decreasing trend in modelled boundary layer heights in winter. This suggests that boundary layer height is an important variable in explaining the build-up at low altitudes although it has little effect higher in the atmosphere and far from continent.

(iv) Using winds as well as boundary layer heights from only one year eliminates the build-up. This suggests that large-scale winds and boundary layer heights are the principal drivers of the build-up with boundary layer heights dominant for the lower atmosphere over continent and winds dominant elsewhere.

6. Acknowledgments

This work has been done within the framework of the EU project CARBOEUROPE. Many thanks to RAMCES people and others, who do their best for measure disponibility in every side of

Europe. CHIMERE is a model developed by IPSL, INERIS and LISA. Part of the implementation of CHIMERE-CO_2 has been supported through the French Environment and Energy Management Agency (ADEME) and the French Atomic Energy Commission (CEA).

References

Baker, D. F., Doney, S. C. and Schimel, D. S. 2006. Variational data assimilation for atmospheric CO_2. *Tellus* **58B**, 359–365.

Bessagnet, B., Hodzic, A., Vautard, R., Beekmann, M., Rouil, L. and co-authors. 2004. Aerosol modeling with CHIMERE—first evaluation at continental scale. *Atmos. Environ.* **38**, 2803–2817.

Bousquet, P., Gaudry, A., Ciais, P., Kazan, V., Monfray, P. and co-authors. 1996. Atmospheric concentration variations recorded at Mace-Head, Ireland, from 1992 to 1994. *Phys. Chem. Earth* **21**, 477–481.

Canadell, J. G., Le Quéré, C., Raupach, M., Field, C. B., Buitenhuis, E. T. and co-authors. 2007. Contributions to accelerating atmospheric CO2 growthfrom economic activity, carbon intensity and efficiency of natural sinks. *Proc. Natl. Acad. Sci. U.S.A.* **104**, 10 288–10 293.

Chan, D., Yuen, C. W., Higuchi, K., Shashkov, A., Liu, J. and co-authors. 2004. On the CO_2 exchange between the atmosphere and the biosphere: the role of synoptic and mesoscale processes. *Tellus* **56B**, 194–212.

Chevallier, F., Viovy, N., Reichstein, M. and Ciais, P. 2006. On the assignment of prior errors in Bayesian inversions of CO2 surface fluxes. *Geophys. Res. Lett.* **33**(13), L13802, doi:10.1029/2006GL026496.

Ciais, P., Reichstein, M., Viovy, N., Granier, A., Ogée, J. and co-authors. 2005. Europe-wide reduction in primary productivity caused by the heat and drought in 2003. *Nature* **437**, 529–533.

Dargaville, R. J., Law, R. M. and Pribac, F. 2000. Implications of interannual variability in atmospheric circulation on modeled CO_2 concentrations and source estimates. *Global Biogeochem. Cycles* **14**, 931–943.

Eckhardt, S., Stohl, A., Wernli, H., James, P., Foster, C. and co-authors. 2003. A 15-year climatology of warm Conveyor belts. *J. Climate* **17**, 218–237.

Geels, C., Gloor, M., Ciais, P., Bousquet, P., Peylin, P. and co-authors. 2007. Comparing atmospheric transport models for future regional inversions over Europe, Part 1. Mapping the atmospheric CO_2 signals. *Atmos. Chem. Phys.* **7**, 3461–3479.

Grell, G. A., Dudhia, J. and Stauffer, D. R. 1994. A description of the fifth-generation Penn State/NCAR mesoscale model (MM5). NCAR Technical Note NCAR/TN-398+STR, 117 pp.

Gurney, K. R., Law, R. M., Denning, A. S., Rayner, P. J., Baker, D. and co-authors. 2002. Towards robust regional estimates of CO_2 sources and sinks using atmospheric transport models. *Nature* **415**, 626–630.

Hauglustaine, D. A., Hourdin, F., Jourdain, L., Filiberti, M.-A., Walters, S. and co-authors. 2004. Interactive chemistry in the Laboratoire de Meteorologie Dynamique general circulation model: description and background tropospheric chemistry evaluation. *J. Geophys. Res.* **109**, D04314, doi:10.1029/2003JD003957.

Honoré, C., Rouil, L., Vautard, R., Beekmann, M., Bessagnet, B. and co-authors. 2008. Predictability of European air quality: assessment of 3 years of operational forecasts and analyses by the PREV'AIR system. *J. Geophys. Res.* **113**, D04301, doi:10.1029/2007JD008761.

Jacob, D. J., Prather, M. J., Rasch, P. J., Shia, R.-L. and Balkanski, Y. J. 1997. Evaluation and intercomparison of global atmospheric transport models using 222Rn and other short lived tracers. *J. Geophys. Res.* **102**, 5953–5970.

Jung, M., Le Maire, G., Zaehle, S., Luyssaert, S., Vetter, M. and co-authors. 2007. Assessing the ability of three land ecosystem models to simulate gross carbon uptake of forests from boreal to Mediterranean climate in Europe. *Biogeosciences* **4**, 647–656.

Krinner, G., Viovy, N., de Noblet-Ducoudré, N., Ogée, J., Friedlingstein, P. and co-authors. 2005. A dynamic global vegetation model for studies of the coupled atmosphere-biosphere system. *Global Biogeochem.Cycles* **19**, GB1015.

Law, R. M., Peters, W., Rödenbeck, C. and TRANSCOM contributors. 2008. TransCom model simulations of hourly atmospheric CO_2: experimental overview and diurnal cycle results for 2002. *Global Biogeochem. Cycles* **22**, GB3009, doi:10.1029/2007GB003050.

Lin, J. C. and Gerbig, C. 2005. Accounting for the effect of transport errors on tracer inversions. *Geophys. Res. Lett.* **32**, L01802, doi:10.1029/2004GL021127.

Lokoshchenko, M. A. and Elansky, N. F. 2006. Dynamics of surface-air pollution during the passage of a cold front. *Izvestiya Atmos. Oceanic Phys.* **42**, 167–175.

Marland, G., Boden, T. A. and Andres, R. J. 2008. Global, regional, and national fossil fuel CO_2 emissions. In: *Trends: A Compendium of Data on Global Change.*, Carbon Dioxide Information Analysis Center, Oak Ridge National Laboratory, U. S. Department of Energy, Oak Ridge, Tenn., USA.

Matulla, C., Schoner, W., Alexandersson, H., von Storch, H. and Wang, X. L. 2007. European storminess: late nineteenth century to present. *Climate Dyn.* **31**, 125–130.

Patra, P., Law, R. M., Peters, W., Rödenbeck, C., Takigawa, M. and TRANSCOM contributors. 2008. TransCom model simulations of hourly atmospheric CO_2: analysis of synoptic scale variations for the period 2002–2003. *Global Biogeochem. Cycles* **22**, GB4013, doi:10.1029/2007GB003081.

Piao, S., Ciais, P., Friedlingstein, P., Peylin, P., Reichstein, M. and co-authors. 2008. Net carbon dioxide losses of northern ecosystems in response to autumn warming. *Nature* **451**, 49–52.

Ramonet, M., Ciais, P., Schmidt, M., Chevallier, F., Kazan, V. and co-authors. 2009. A recent build-up of atmospheric CO_2 over Europe. Part 1: Observed signals and possible explanations. *Tellus* **61B**, doi:10.1111/j.1600-0889.2009.00442.x.

Rayner, P. J., Law, R. M., Allison, C. E., Francey, R. J. and Pickett-Heaps, C. 2008. Interannual variability of the global carbon cycle (1992–2005) inferred by inversion of atmospheric CO_2 and $\delta^{13}CO_2$ measurements. *Global Biogeochem. Cycles* **22**, GB3008, doi:10.1029/2007GB003068.

Rödenbeck, C., Houweling, S., Gloor, M. and Heimann, M. 2003. CO_2 flux history 1982-2001 inferred from atmospheric data using a global inversion of atmospheric transport. *Atmos. Chem. Phys.* **3**, 1919–1964.

Schmidt, H., Derognat, C., Vautard, R. and Beekmann, M. 2001. A comparison of simulated and observed ozone mixing ratios for the summer of 1998 in Western Europe. *Atmos. Environ.* **35**, 6277–6297.

Smits, A., Klein Tank, A. M. G. and Konnen, G. P. 2005. Trends in storminess over the Netherlands, 1962–2002. *Int. J. Climatol.* **25**, 1331–1344.

Szegvary, T., Leuenberger, M. C. and Conen, F. 2007. Predicting terrestrial 222Rn flux using gamma dose rate as a proxy. *Atmos. Chem. Phys.* **7**, 2789–2795.

Takahashi, T., Sutherland, S. C., Sweeney, C., Poisson, A., Metzl, N. and 2002. Global sea-air CO2 flux based on climatological surface ocean pCO_2, and seasonal biological and temperature effects. *Deep-Sea Res. Part II. Topical Stud. Oceanogr.* **49**, 1601–1622.

Thoning, K. W., Tans, P. P. and Komhyr, W. D. 1989. Atmospheric carbon dioxide at Mauna Loa Observatory. 2: analysis of the NOAA/GMCC data, 1974–1985. *J. Geophys. Res.* **94**, 8549–8565.

van Aardenne, J. A., Dentener, F. J., Olivier, J. G. J., Peters, J. A. H. W. and Ganzeveld, L. N. 2005. The EDGAR 3.2 Fast track 2000 dataset (32FT2000). JRC Technical report, Joint Research Centre (JRC), Ispra, Italy.

van Loon, M., Vautard, R., Schaap, M., Bergstrom, R., Bessagnet, B. and co-authors. 2007. Evaluation of long-term ozone simulations from seven regional air quality models and their ensemble. *Atmos. Environ.* **41**, 2083–2097.

Vetter, M., Churkina, G., Jung, M., Reichstein, M., Zaehle, S. and co-authors. 2008. Analyzing the causes and spatial pattern of the European 2003 carbon flux anomaly using seven models. *Biogeosciences* **5**, 561–583.

Wanninkhof, R. 1992. Relationship between wind speed and gas exchange. *J. Geophys. Res.* **97**, 7373–7382.